Near Surface Geophysics Challenges, a Snapshot

Aldo Vesnaver

Khalifa University of Science and Technology – Petroleum Institute, Petroleum Geoscience Department, Sas Al-Nakhl, P.O. Box 2533, Abu Dhabi, United Arab Emirates

Received June 15, 2017; Accepted June 22, 2018

Abstract: Near surface complexities have been and remain the toughest challenge for oil and gas exploration on land, where most of the proven reserves are located. The same complexities are present for environmental applications, such as CO_2 sequestration or the quest for deep aquifers. In this paper I review a few of these continuing challenges and present examples of recent techniques and technologies that may contribute to their solution.

Keywords: Near surface, seismic, integration, uphole, geostatistics

1 Introduction

The paradox of most geophysical surveys, especially seismic ones, is the difficulty in resolving the shallowest inhomogeneities, unlike the deeper targets. Something similar happens when taking a photograph of a landscape with a hand in the foreground: the landscape may be quite sharper than our own fingers, when the fingers are actually quite close to the camera lens. A practical solution to keep both parts of the photograph in focus might be taking several snapshots with increasing focal distances, using the zoom, and combining them with image processing. This approach is often used in resistivity and gravity surveys. For seismic surveys, combined recording systems have been introduced in past decades by building arrays of synchronized sources with different frequency bands and precise spatial patterns. In the current decade, blended sources generalized this concept by allowing for arbitrary source number, type, location, and synchronization (see Beasley 2008, Berkhout *et al*. 2009, Pecholcs *et al.* 2010, and Berkhout 2012, among many others). However, in seismic acquisition for hydrocarbon exploration or CO_2 geological storage, multiple deployments of sources and receivers with different penetration and resolution may be quite demanding, especially when it comes to 3D surveys. Some recent single-sensor, single-source surveys (also called 4S surveys)

Corresponding author: aldo.l.vesnaver@gmail.com

DOI: 10.7569/JSEE.2018.629506

showed dramatic improvements in land data quality (see El-Emam and Khalil 2012, Granser *et al.* 2015), but a significant increase in costs, a longer processing time, and a booming data size. For these reasons, in this paper I review the restrictions of some classical approaches and provide a snapshot of the current trends in research and development that are aimed at improving near surface characterization at more affordable acquisition costs.

2 A Classic Approach: The Upholes' Challenge

About two-thirds of the seismic energy introduced into the Earth by a vibrator seismic source is converted into surface waves (Pursey 1955, Miller and Pursey 1955). For decades, the practical solution for attenuating these waves, called ground roll, has been arranging both sources and receivers into 2D or 3D arrays. This configuration helps enhance their directivity along the vertical direction where reflections of P-waves are stronger (see Cordsen *et al.* 2000, Vermeer 2012, among many others). However, when it comes to seismic surveys in arid deserts, where most of the Earth's proven reserves are located, using arrays introduces serious drawbacks in the vertical resolution. Figure 1 depicts the relative size of a vibrator (about 10 m) versus common array size and interval (50 and 25 m, respectively). These lengths are comparable with the dominant wavelengths of seismic signals when assuming a frequency peak of 40 Hz in the seismic source. As near-surface velocity may

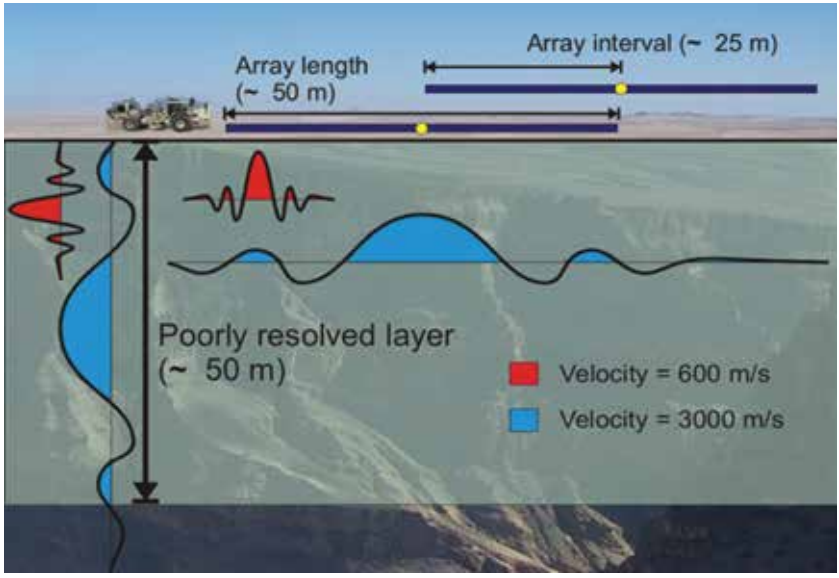

Figure 1 Visual comparison among the size of seismic wavelet, receiver arrays, a vibrator truck, and the shallowest 50m of a real outcrop.

DOI: 10.7569/JSEE.2018.629506

switch abruptly due to shallow complexities from 600 to 3000 m/s, the dominant wavelengths may range from 15 to 80 m or so. This happens, for example, in the Middle Eastern deserts where carbonate *jebels* outcropping among sandy dunes cause large and sharp velocity changes. In these conditions, near surface modelling becomes very challenging, especially when adopting a single geophysical method, and the result is a significant information gap (see Pecholcs *et al.* 2001, Vesnaver 2004).

A classical method for improving the estimation of shallow P velocities is an uphole survey. Historically, when dynamite was a standard seismic source, upholes were recorded at the intersections of 2D lines within a regional survey to improve the ties of signals and velocity models. Their interpolation is still used for building near surface models at a large scale, for example, for integrating adjacent 3D surveys in a large country like Saudi Arabia (Bridle *et al.* 2007, Bridle 2008). Vesnaver *et al.* (2006) showed that for a sparse uphole distribution, only velocity anomalies with a size double that of the average uphole distance can be approximately recovered. This is what may be predicted by the Nyquist theorem for a regular sampling.

An additional challenge for using upholes comes when a time-lapse seismic survey is planned. The weathered layer, from 0 to 50m depth, is the most sensitive to weather variations. Seasonal effects (e.g. rain, snow, drought) may significantly alter the moisture content and the water table level in the weathered layer. As a result, consistent shallow velocities become season-dependent; Soroka *et al.* (2005a, b) experienced repeatability errors on the order of 12% of a 4D pilot experiment in the United Arab Emirates. Bakulin *et al.* (2016) showed that Normalized Root-Mean-Square (NRMS) differences greater than 45% are observed in buried receivers at a depth of 70 m, a usual depth for upholes, unless a major processing effort is spent to remove the noise. Using 1000 shallow wells located 50m apart in a regular grid, they were able to reduce the NRMS difference to only 5%. Unfortunately, this is a unique case as typical surveys have just one measurement, so this range for the NRMS variability is a reasonable guess for the repeatability of uphole records in general.

To better quantify the seasonal effects on uphole-based interpolations, I further elaborated the synthetic example presented by Vesnaver *et al.* (2006). Figure 2 shows four different models for a weathering layer with velocities ranging from 900 to 1700 m/s. The background is a sinusoidal function, in x and y directions, with a wavelength of 10 km. In model A, the black circles indicate the upholes' survey locations. In models B, C, and D, random velocity perturbations were added with velocity errors of ±100, ±300, and ±900 m/s. Relative to the average velocity of the background, 1300 m/s, these perturbations correspond to percentages of 8%, 23%, and 69%. While the 69% variation in the last case (model D) is quite extreme, the perturbations in models B and C are in the range expected for seasonal changes.

For the next step in using uphole survey data, the data processing step, we can ignore the noise contribution in each of the resulting data sets. The noise contribution is obtained by sampling the four models at the uphole locations. An effective

DOI: 10.7569/JSEE.2018.629506

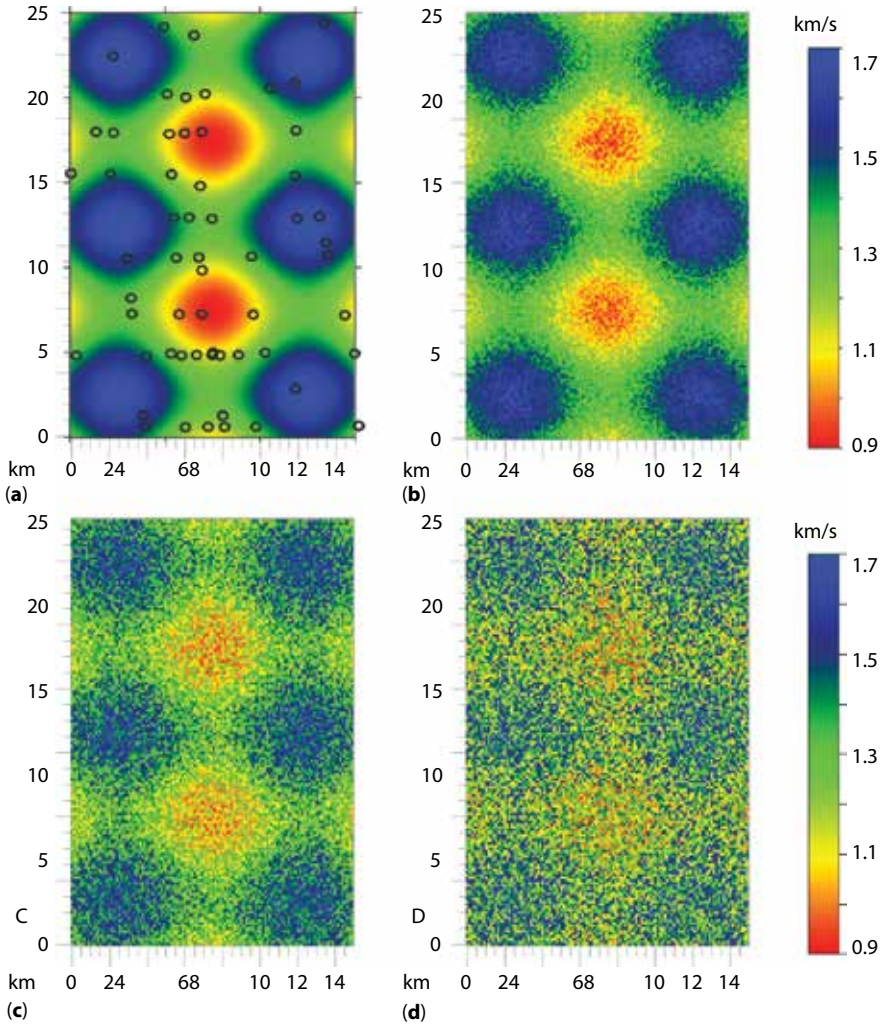

Figure 2 Velocity models for a shallow layer with sinusoidal functions in the x and y directions without perturbations (**a**) and with absolute perturbations of 100 m/s (**b**), 300 m/s (**c**), and 900 m/s (**d**). The black circles in model A indicate the uphole locations where the velocity fields are sampled.

technique for estimation of the noise is provided by their variograms (Figure 3). The variogram value at the origin, called nugget, is ideally zero for noise-free data, as highlighted by the red circle for model A; in Figure 3, the nugget grows larger for the other three models. Another possible use of variograms is the interpretation of their range, or the distance when the rise of the variogram function stops

DOI: 10.7569/JSEE.2018.629506

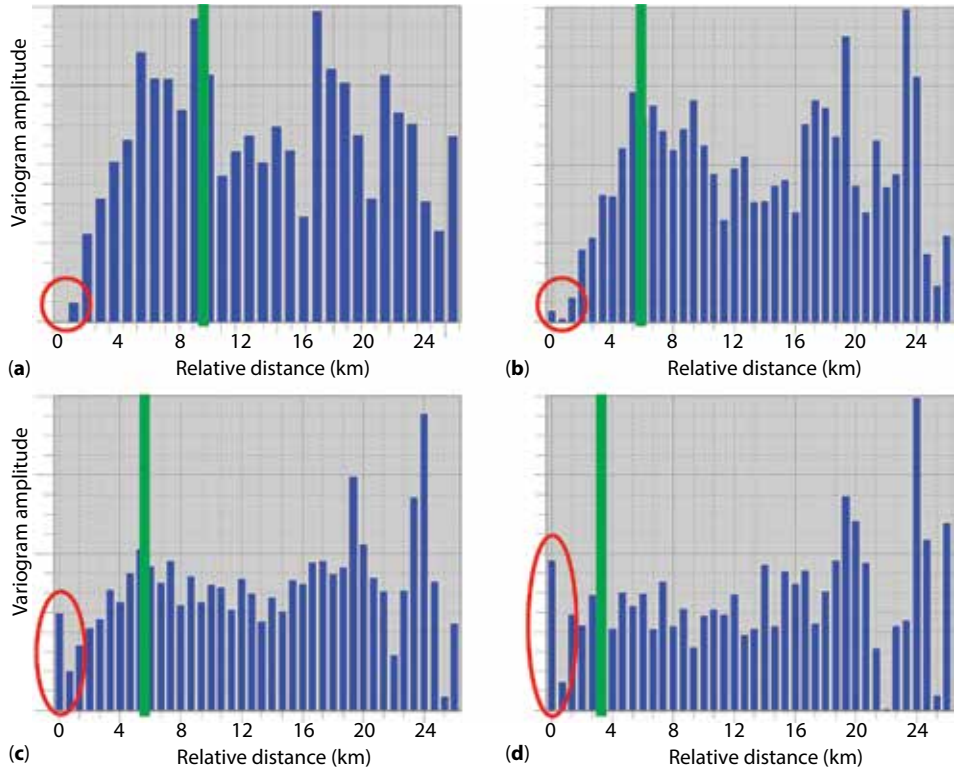

Figure 3 Variograms obtained by the sample velocity values of the models in Figure 2.

and reaches a plateau. In Figure 3, reasonable range values are indicated by the vertical green lines. Once again, we notice that the noise-free model A suggests a range between 5 and 10 km; the latter is exactly the wavelength of the background velocity field, while such a distance decreases when the noise is larger. Consequently, interpolation by kriging (see Dubrule 2003), normally based on the range as a key parameter, would be flawed from the very beginning, independent from the uphole location. Actual kriging interpolation provides the smooth models in Figure 4, where the high-frequency noise contribution is gone, but the distortion of the remaining low-frequency components is acceptable only for models A and B, namely where velocity perturbations do not exceed 8%.

3 The Integration Challenge: Mixing Classic Techniques with Modern Methods

A general consensus exists about geophysical data integration as a key tool for improving our Earth models. For the near surface, various studies have been

DOI: 10.7569/JSEE.2018.629506

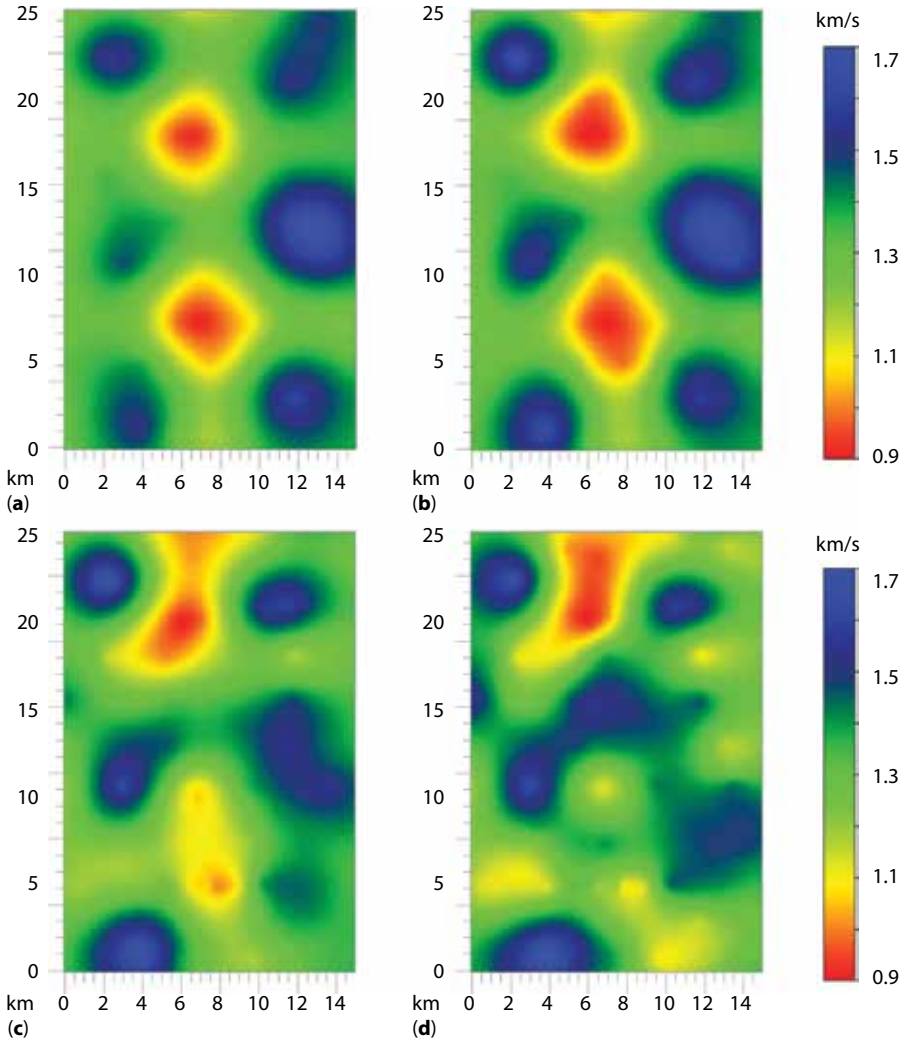

Figure 4 Interpolated velocity fields by kriging for the velocities sampled in the models in Figure 2 using the range and nugget parameters interpreted in Figure 3.

published linking two methods at a time, such as resistivity with seismic data (Gallardo and Meju 2003), gravity with magneto-telluric data (Krieger *et al.* 2002), gravity and magnetic data (Fregoso and Gallardo 2009), and seismic with electro-magnetic (Zerilli *et al.* 2016) or magneto-telluric data (Gallardo and Meju 2007, Molodtsov *et al.* 2013), and less frequently three or more methods together (Dell'Aversana 2001, Dell'Aversana *et al.* 2002, Colombo and De Stefano 2007,

DOI: 10.7569/JSEE.2018.629506

Colombo and Keho 2010, Li *et al.* 2011). Vesnaver *et al.* (2009) applied the concept of clustering, often used for reservoir characterization, to link several seismic attributes with rock parameters. A strength of this approach is its ability to build a shared Earth model by measurements that are heterogeneous in terms of physical phenomena, resolution, and sampling density. However, a clustering weakness is the subjective choice of the cluster number and the relative weights for each measurement type (see Jain and Dubes 1988). As a result, we can expect a variety of solutions based on personal preferences or "*a priori*" information available to the interpreter.

Figure 5 (top) shows a bar chart with the variogram of shallow velocities obtained by upholes and (bottom) the relative distribution of distances between uphole couples. When the fold decreases below the average for large offsets, the corresponding variogram values become unreliable. The vertical red bar is a possible interpretation for the range, which is quite questionable. The velocity values are very noisy because the nugget is extremely high. This fact may indicate either an extreme heterogeneity within a small distance range or, more probably, measurements taken in different seasons, which may drastically affect the weathering properties.

Figure 6 (left) shows the variogram of Bouguer anomalies for a 3D gravity survey acquired in the Arabian Peninsula in the same region studied by Vesnaver *et al.* (2006). The nugget is quite small and the variogram function is smooth, with a range at about 32 km, which could be approximated by a spherical or

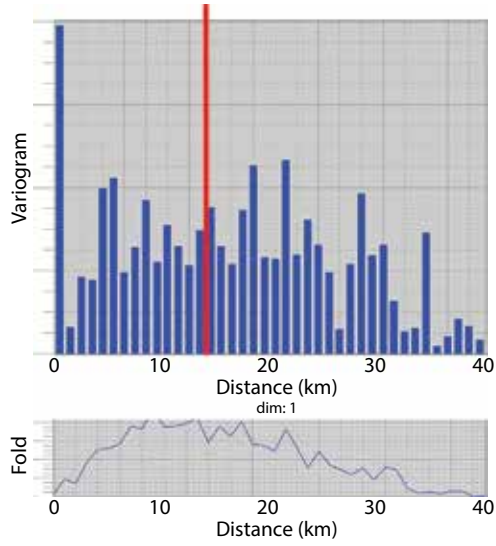

Figure 5 Variogram of uphole velocities (top) and the variogram data fold (bottom). The red vertical bar indicates the interpreted range.

DOI: 10.7569/JSEE.2018.629506

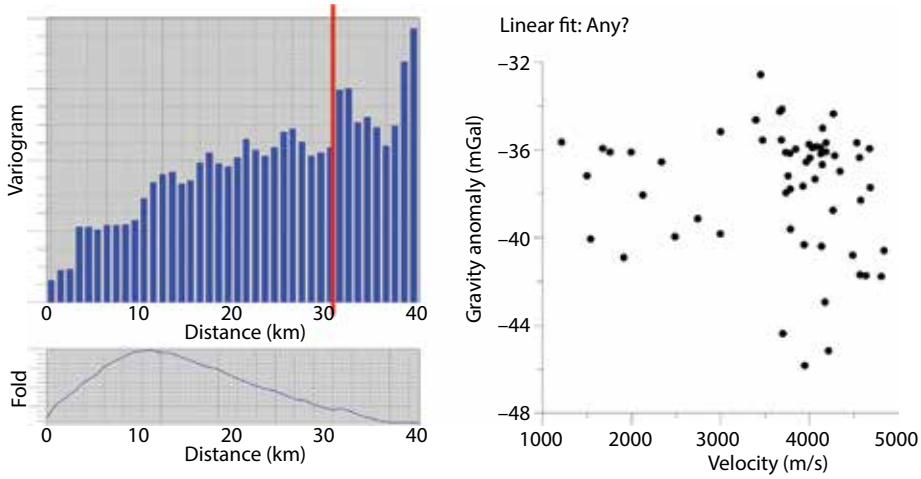

Figure 6 Variogram of gravity data acquired in the same area of upholes (top left), the variogram data fold (left bottom), and the cross-plot of velocities versus gravity anomalies at the same location (right). The red vertical bar indicates the interpreted range.

exponential variogram model (see, e.g., Dubrule 2003). Despite the good data quality suggested by nugget and range, the cross-plot of gravity anomalies versus shallow uphole velocities is very poor (Figure 6, right); the scattered points cannot be fairly interpolated by any line to build an empirical relationship between these two parameters. Thus, the type of inhomogeneities in the near surface requires a larger number of parameters (or degrees of freedom) to be properly modelled in a similar manner as for reservoir characterization, where density, fluid saturation, Q factor, porosity, and other rock properties are also estimated for accurate reservoir modelling.

From the same study, Figure 7 shows a very different trend for the viscosity parameter. This parameter describes the anelastic response of the ground to a vibrator seismic source. It is normally provided in land acquisition reports and files, but is rarely used in standard processing, despite its proven effectiveness (Al-Ali *et al*. 2003, Ley *et al*. 2006). It might be approximated by a Gaussian variogram model, but its key feature is a significant noise pedestal, which would suggest the presence of significant random noise. Unlike the cross-plot in Figure 5, the cross-plot of viscosity and shallow velocity falls along a trend, although there is significant scatter among the points.

In Figure 8, I compare a third parameter to velocity. On the left, it shows the variogram obtained by the Landsat TM Band 5 satellite imagery, i.e. short-wave infrared with wavelengths ranging from 1.55 to 1.75 μm. This band was chosen because it clearly highlighted the boundaries of shallow formations controlled by upholes and field reports. The nugget for this data is smaller and the shape is even

DOI: 10.7569/JSEE.2018.629506

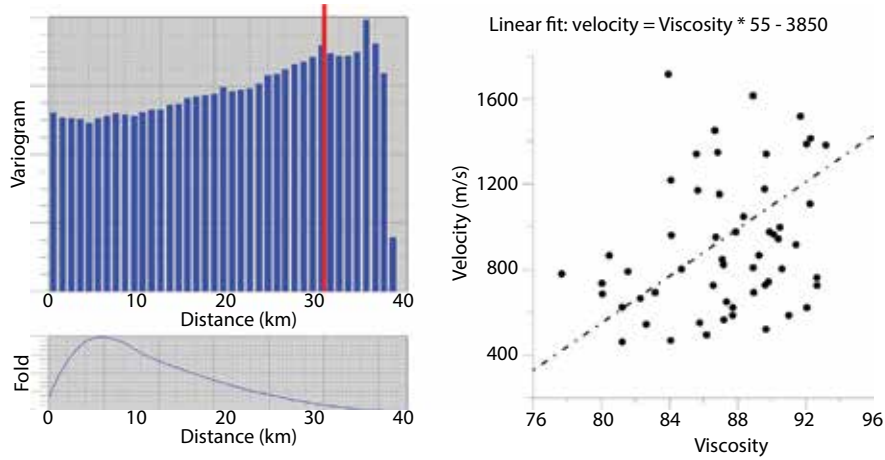

Figure 7 Variogram of viscosity data acquired in the same area of upholes (top left), the variogram data fold (left bottom), and the cross-plot of viscosity versus velocities at the same locations (right). The red vertical bar indicates the interpreted range.

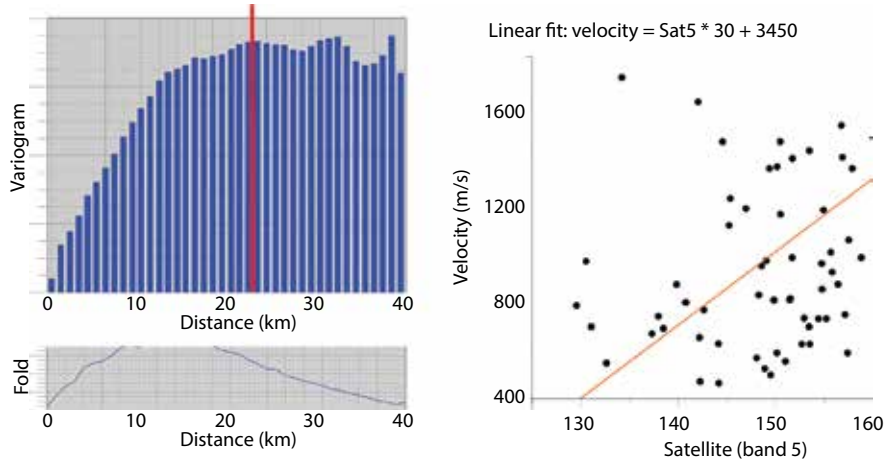

Figure 8 Variogram of satellite data acquired in the same area of upholes (top left), the variogram data fold (left bottom), and the cross-plot of satellite data versus velocities at the same locations (right). The red vertical bar indicates the interpreted range.

smoother than for the gravity data in Figure 5, suggesting a low noise contamination. In fact, the cross-plot with shallow velocities displays a lower scattering with respect to the others, but still a significant one. The explanation for these poor correlations is provided by the uphole velocity variogram (Figure 5) where we notice a huge nugget component probably due to several velocity values acquired

DOI: 10.7569/JSEE.2018.629506

in different seasons. Whatever the reason, in this case, the integration of satellite, vibrator plate, and gravity with upholes is compromised by the low quality of the upholes.

4 Recent Advances and Perspectives in Land Geophysical Acquisition

When integrating seismic and non-seismic methods, the resolution of non-seismic methods is often perceived as lower. However, Colombo *et al.* (2016a, b) showed that helicopter-borne transient electromagnetic systems may acquire data with a lateral resolution of 2.7m along the flight line, which is higher than the related seismic survey. As the electromagnetic signal penetration reaches 400-500m, the near surface is characterized very well. Also, in desert areas where the water table may reach a comparable depth, the largest velocity contrasts are normally found above the water table. The quality of the seismic imaging processed by a consistent Earth model, integrating the information provided by the electromagnetic data, was remarkably improved.

Surface waves provide the strongest seismic signal in terms of energy, but its key information is about S velocity in the shallowest layer. For this reason, it has been considered as noise by explorationists in most cases, but as an ideal signal by civil engineers and environmental geophysicists (see Socco and Strobbia 2004, Socco *et al.* 2010). Bridging S and P velocity anomalies in the near surface may be facilitated by building a consistent geological model. Duret *et al.* (2016) proposed an integrated workflow, including first-arrival travel time inversion and multi-offset phase analysis (Strobbia and Foti 2006). The significant advantage of their approach is filling the near surface information gap present in a standard, spatially-coarse seismic survey by using surface wave analysis and, thereby, linking them in the depth range that they cover with a good signal reliability. Re *et al.* (2010) preferred a joint tomographic inversion using grids with a different resolution for surface and body waves, but imposing constraints about the ratio between P and S velocities.

Full-waveform inversion has been evolving rapidly in the last few years, moving from synthetic examples to successful pilot tests with marine data (where acoustic models may be acceptable) and to a few pioneering applications to land data (where a visco-elastic modelling is needed). Mei *et al.* (2014) presented a pioneering full 3D survey acquired in Alaska, where acoustic full-waveform inversion contributed to imaging quality improvement. Kim and Tsingas (2014) carried out a relevant experiment involving blended seismic sources with different frequency bands. Shi *et al.* (2016) presented a 3D example of elastic joint inversion of surface and body waves.

5 Conclusions

The progress in land data processing for modelling and compensating the near surface distortions of seismic signals has been remarkable in the last decade. The

DOI: 10.7569/JSEE.2018.629506

quantitative integration of non-seismic methods made a major contribution to improve near-surface modeling, although further studies are needed to provide a more solid theoretical background to methods, such as clustering, or when heterogeneous parameters are involved, such as density, elasticity parameters, and resistivity. The analysis of the quality of available data is the first step for a possible integration with other data to ultimately build a shared Earth model for the near surface. Variograms are a classic, powerful tool for this.

When remaining in the seismic processing realm, full-waveform inversion seems to be the final answer to the evergreen problem of integrating body and surface waves. The recent advances in acquisition techniques (such as broadband systems and single-sensor single-receiver recordings) are providing the ideal input for further improvements in joint high-resolution imaging of both shallow and deep targets. We can expect spectacular results in the near future, as soon as the massive computing power required is available at affordable costs and the existing software infrastructure is adjusted to allow for the massive increase of new data to process.

References

1. M. Al-Ali, R. Hastings-James, M. Makkawi, and G. Korvin, Vibrator attribute leading velocity estimation. *The Leading Edge* **22**, 400–405 (2003).
2. A. Bakulin, R. Smith, E. Hemyari, A. Ramadan, M. Jervis, and C. Saragiotis, Processing and repeatability of 4D buried receivers in a desert environment. Expanded Abstracts, SEG Annual Meeting, 5405–5409 (2016).
3. A. J. Berkhout, G. Blacquiere, and D. J. Vershuur, The concept of double blending: combining incoherent shooting with incoherent sensing. *Geophysics* **74**, A59–A62 (2009).
4. A. J. Berkhout, Blended acquisition with dispersed blended source arrays. *Geophysics* **77**, A19–A23 (2012).
5. C. J. Beasley, A new look at marine simultaneous sources. *The Leading Edge* **27**, 914–917 (2008).
6. R. Bridle, R. Ley, and A. Al-Mustafa, Near-surface models in Saudi Arabia. *Geophysical Prospecting* **55**, 779–792 (2007).
7. R. Bridle, Gaining a geostatistical advantage in bear-surface modeling. SEG Expanded Abstracts, 1218–1222 (2008).
8. D. Colombo and M. De Stefano, Geophysical modeling via simultaneous joint inversion of seismic, gravity, and electromagnetic data: Application to prestack depth imaging. *The Leading Edge* **26**, 326–331 (2007).
9. D. Colombo and T. Keho, The non-seismic data and joint inversion strategy for the near surface solution in Saudi Arabia. Expanded Abstracts, SEG Annual Meeting, 1934–1938 (2010).
10. D. Colombo, G. McNeice, D. Rovetta, E. Sandoval-Curiel, E. Turkoglu, and A. Sena, High-resolution velocity modeling by seismic-airborne TEM joint inversion: A new perspective for near-surface characterization. *The Leading Edge* **35**, 977–985 (2016a).
11. D. Colombo, D. Rovetta, E. Turkoglu, G. McNeice, E. Sandoval-Curiel, and A. Sena, Seismic-airborne TEM joint inversion for near-surface velocity modeling in a complex wadi. Expanded Abstracts, SEG Annual Meeting, 927–931 (2016b).

DOI: 10.7569/JSEE.2018.629506

12. A. Cordsen, M. Galbraith, and J. Peirce, Planning land 3D seismic surveys. SEG, Tulsa, 204 pages (2000).
13. P. Dell'Aversana, Integration of Seismic, MT, and gravity data in a thrust belt interpretation. *First Break* **19**, 335–341 (2001).
14. P. Dell'Aversana, S. Morandi, and M. Buia, Pre-stack depth migration of "Global Offset" data integrated with high resolution magnetotelluric and gravity. Expanded Abstracts, SEG Annual Meeting, 556–559 (2002).
15. O. Dubrule, Geostatistics for seismic data integration in Earth models. SEG/EAGE, Distinguished Instructor Series, 6, 279 pp, (2003).
16. F. Duret, F. Bertin, K. Garceran, R. Sternfels, T. Bardainne, N. Deladerriere, and D. Le Meur, Near-surface velocity modeling using a combined inversion of surface and refracted P-waves. *The Leading Edge* **35**, 946–951 (2016).
17. A. El-Emam and S. Khalil, Maximizing the value of Single-Sensor measurements, Kuwait experience. Expanded Abstracts, SEG Annual Meeting, 1–5 (2012).
18. E. Fregoso and L. A. Gallardo, Cross-gradients joint 3D inversion with applications to gravity and magnetic data. *Geophysics* **74**, L31–L42 (2009).
19. L. A. Gallardo and M. A. Meju, Characterization of heterogeneous near-surface materials by joint 2D inversion of dc resistivity and seismic data. *Geophysical Research Letters* **30**, 1658 (2003).
20. L. A. Gallardo and M. A. Meju, Joint two-dimensional cross-gradient imaging of magnetotelluric and seismic traveltime data for structural and lithological classification. *Geophysical Journal International* **169**, 1261–1272 (2007).
21. H. Granser, B. Novotny, L. Fava, and B. Vermeulen, Recent 4S High Fold 3D Seismic acquisitions in the Abu Dhabi foreland of the Oman Mountains. ADIPEC Expanded Abstracts, Society of Petroleum Engineers, doi: 10.2118/177534-MS (2015).
22. A. K. Jain and R. C. Dubes, Algorithms for clustering data. Prentice Hall, Englewood Cliffs, 320 pp (1988).
23. Y. S. Kim and C. Tsingas, Elastic full waveform inversion on land data acquired with dispersed source arrays. Expanded Abstracts, SEG Annual Meeting, 1007–1011 (2014).
24. M. H. Krieger, C. H. Henke, and A. Zerilli, Gravity and magnetotelluric modelling of salt structures for improved seismic imaging. Extended Abstracts, EAGE Annual Meeting (2002).
25. R. Ley, W. Adolfs, R. Bridle, M. Al-Homaili, A. Vesnaver, and P. Ras, Ground viscosity and stiffness measurements for near surface seismic velocity. *Geophysical Prospecting* **54**, 751–762 (2006).
26. X. Li, Y. Li, X. Meng, and M. A. Meju, Joint multi-geophysical inversion: Effective model integration, challenges and directions for future research. International Workshop on Gravity, Electrical and Magnetic Methods and Their Applications, Beijing, China, 37–37 (2011).
27. J. Mei, S. Ahmed, A. Searle, and C. O. Ting, Application of full waveform inversion on Alaska land 3D survey. Expanded Abstracts, SEG Annual Meeting, 981–986 (2014).
28. G. F. Miller and H. Pursey, On the partition of energy between elastic waves in a semi-infinite solid. Proceedings of the Royal Society **233**, Section A, issue 1192 (1955).
29. D. M. Molodtsov, V. N. Troyan, Y. V. Roslov, and A. Zerilli, Joint inversion of seismic traveltimes and magnetotelluric data with a directed structural constraint. *Geophysical Prospecting* **61**, 1218–1228 (2013).

DOI: 10.7569/JSEE.2018.629506

30. P. I. Pecholcs, L. LaFreniere, S. Hubbel, V. Kozyrev, I. Korotkov, and A. Zhukov, Spatially fixed patterns for resolving large magnitude short wavelength statics and more. EAGE Extended Abstracts, IS-4 (2001).
31. P. I. Pecholcs, S. K. Lafon, T. Al-Ghamdi, H. Al-Shammery, P. G. Kelamis, S. X. Huo, O. Winter, J. B. Kerboul, and T. Klein, Over 40,000 vibrator points per day with real-time quality control: opportunities and challenges. Expanded Abstracts, SEG Annual Meeting, 111–115 (2010).
32. H. Pursey, The power radiated by an electromechanical wave source. Proceedings of the Physical Society **69**, Section B, 139–144 (1955).
33. S. Re, C. Strobbia, M. De Stefano, and M. Virgilio. Simultaneous joint inversion of refracted and surface waves. Expanded Abstract, SEG Annual Meeting, 1915–1918 (2010).
34. J. Shi, M. De Hoop, F. Faucher, and H. Calandra, Elastic full-waveform inversion with surface and body waves. Expanded Abstract, SEG Annual Meeting, 1120–1124 (2016).
35. L. V. Socco and C. Strobbia, Surface-wave method for near-surface characterization: a tutorial. *Near surface geophysics* **2**, 165–185 (2004).
36. L. V. Socco, S. Foti, and D. Boiero, Surface wave analysis for building near-surface velocity models – Established approaches and new perspectives. Geophysics 75, &%A83-75A102 (2010).
37. W. L. Soroka, P. Melville, E. Kleiss, M. Al-Jenaibi, H. H. Hafez, A. B. Al-Jeelani, A. Modavi, and J. S. Gomes, Successful 4D monitoring and saturation in a giant Middle Eastern carbonate reservoir: ADCO Phase 1 pilot results. In: Methods and applications in reservoir geophysics, D. H. Johnston (ed.), Tulsa: SEG (2005a).
38. W. L. Soroka, P. Melville, E. Kleiss, M. Al-Jenaibi, A. B. Al-Jeelani, H. H. Hafez, and A. Modavi, Successful pilot onshore Abu Dhabi shows that 4D can monitor fluid changes in a giant Middle East carbonate field. Expanded Abstracts, SEG Annual Meeting, 2430–2433 (2005b).
39. C. Strobbia, and S. Foti, Multi-offset phase analysis of surface waves data (MOPA). *Journal of Applied Geophysics* **59**, 300–313 (2006).
40. G. Vermeer, 3D seismic survey design. SEG, Tulsa, 342 pages (2012).
41. A. Vesnaver, The near-surface information gap for time and depth imaging. *Geophysical Prospecting* **52**, 653–661 (2004).
42. A. Vesnaver, R. Bridle, B. Henry, R. Ley III, R. Rowe, and A. Wyllie, Geostatistical integration of near-surface geophysical data. *Geophysical Prospecting* **54**, 763–777 (2006).
43. A. Vesnaver, R. Bridle, R. Ley III, and C. Liner, Painting the near surface using geology, geophysics, and satellites. *Geophysics* **74**, B-61–B69 (2009).
44. A. Zerilli, M. P. Buonora, F. Miotti, J.L.S. Crepaldi, and P. T. L. Menezes, Using broadband mCSEM-driven velocity model building to improve complex subsalt imaging. Extended Abstract, EAGE Annual Meeting, doi: 10.3997/2214-4609.201600942 (2016).

DOI: 10.7569/JSEE.2018.629506